Geosci. Model Dev. Discuss., 7, 8361–8397, 2014
www.geosci-model-dev-discuss.net/7/8361/2014/
doi:10.5194/gmdd-7-8361-2014

Geoscientific Model Development Discussions
Open Access

Simulations and parameterisation of shallow volcanic plumes of Piton de la Fournaise, La Réunion Island using Méso-NH version 4-9-3

S. G. Sivia[1,2], F. Gheusi[1], C. Mari[1], and A. Di Muro[3]

[1]Laboratoire d'Aérologie (LA), University of Toulouse and CNRS, UMR5560, Toulouse, France
[2]Laboratoire de l'Atmosphère et Cyclones (LACy), Université de La Réunion, CNRS, Météo-France, UMR 8105, Saint-Denis de La Réunion, France
[3]Laboratoire de Géologie des Systèmes Volcaniques, IPGP, CNRS, UMR 7154, Paris, France

Received: 18 September 2014 – Accepted: 29 October 2014 – Published: 26 November 2014

Correspondence to: F. Gheusi (francois.gheusi@aero.obs-mip.fr)

Published by Copernicus Publications on behalf of the European Geosciences Union.

Abstract

In mesoscale models (resolution ∼ 1 km) used for regional dispersion of pollution plumes, the heat sources, the induced atmospheric convective motions and the volcanic emissions of gases and aerosols are all sub-grid scale processes (mostly true for effusive eruptions) which need to be parameterized. We propose a modified formulation of the EDMF scheme (Eddy Diffusivity-Mass Flux) proposed by Pergaud et al. (2009) which is based on a single updraft. It is used to represent volcano induced updrafts tested for a case study of January 2010 summit eruption of Piton de la Fournaise (PdF) volcano. The validation of this modified formulation using large eddy simulation (LES) focuses on the ability of the model to transport tracer concentrations up to 1–2 km in the lower troposphere as is the case of majority of PdF eruptions. The modelled volcanic plume agrees well with the SO_2 (sulphur dioxide) tracer concentrations found with LES and a sensitivity test performed for the modified formulation of the EDMF scheme emphasizes the sensitivity of the parameterisation to entrainment at the plume base.

1 Introduction

A critical factor in successfully monitoring and forecasting volcanic ash and gases dispersion is the height reached by eruption clouds, which is affected by environmental factors, such as wind shear and atmospheric vertical stability (Glaze and Baloga, 1996; Graf et al., 1999; Bursik, 2001; Tupper et al., 2009). The term “volcanic plume” refers to both the vertical buoyant column of gas/ash above the eruptive vent, and the following horizontal transport of pollutants at the regional scale by the wind flow. The convective scale corresponds to the unstable region where intense but localised sensible and latent heat fluxes released by pyroclasts, gases and lava near eruptive vents generate convection which transports energy and pollutants to high altitudes through buoyant plumes. Throughout the course of this convection mixing of the plume with the atmosphere takes place at different levels of altitude through entrainment and

GMDD
7, 8361–8397, 2014

detrainment. This process allows for the distribution of pollutants over a certain vertical range.

Piton de la Fournaise (PdF) is one of the world's most active volcanoes (Lenat and Bachelery, 1987) with an average of one eruption every eight months in the last fifty years (Peltier et al., 2009). Most of the studies undertaken for deep volcanic injection have been applied to stratospheric injections, which are mostly performed by large explosive volcanoes (comprehensive review by Robock, 2000). However, much less is known about the environmental and atmospheric impacts and fates of volcanic plumes injected into the troposphere (Mather et al., 2003; Delmelle et al., 2002). PdF can create a major source of tropospheric air pollution as was the case during the eruption of April 2007 (Tulet and Villeneuve, 2011). The air-quality standard for ecosystem and human health protection was exceeded for sulphur dioxide (SO_2) at several inhabited locations in the south-west and north-west part of the island (opposite from the location of the eruption) (Viane et al., 2009; Bhugwant et al., 2009; Lesouef et al., 2011).

Simulations of atmospheric plumes from intense heat source points have been performed using Méso-NH (Lafore et al., 1998) model to represent the impact of forest fires on the dynamic and chemistry of the atmosphere. A study by Strada et al. (2012) simulated forest fire plumes at 1 km resolution which showed good agreement with observations where high sensitivity to the atmospheric stability was observed. Simulations of the eruption column dynamics, chemistry dispersal in the proximal environment and the volcanic cloud tracking at regional scale rely on similar numerical and conceptual approaches as the ones used for the study of the forest fire plumes. In kilometric resolution models used for air quality purposes (simulation or forecasts), the localised heat source is diluted in the model grid and hence no convection is explicitly generated.

Several types of atmospheric movements are sub-grid processes, and they are incorporated into atmospheric models through appropriate parameterisation schemes. In order to determine the evolution of volcanic plumes in the atmosphere, numerical models need to consider two different scales:

1. an implicit/convective scale corresponding to the convective plume above the erupting volcano, whose processes are sub-grid even at fine resolutions (> 500 m), and
2. an explicit/dispersion scale that corresponds to the dispersion of the volcanic plume in the atmosphere.

In mesoscale models (resolution ∼ 1 km) used for regional dispersion of pollution plumes, the heat sources, the induced atmospheric convective motions and the volcanic emissions of gases and aerosols are all sub-grid scale processes which need to be parameterized.

In this article we briefly describe an existing sub-grid shallow convection scheme by Pergaud et al. (2009) usually used in the atmospheric model Méso-NH for weather simulations. This scheme is adapted in Sects. 2.2.2 and 2.2.3 such that the size and intensity of the ground heat source provided by the eruption is initialised for modelling the sub-grid updraft. This parameterisation is tested on a 1 dimensional (1-D) single column model (SCM) with a 1 km resolution for an eruption observed at PdF in January 2010. The choice of 1 km resolution for SCM simulations is because it is the target resolution of future forecast models running over Reunion Island. Simultaneously, a three dimensional (3-D) Large Eddy Simulation (LES) is performed (10 m resolution) using the same size and intensity of the eruption as prescribed for the adapted convection scheme. Finally the results of the vertical mass and tracer concentration budgets obtained from SCM are validated against the LES results.

2 Materials and methods

2.1 Description of the January 2010 summit eruption of Piton de la Fournaise

An eruption took place on 2 January 2010 around 10:20 UTC at the summit of Piton de la Fournaise (PdF) located at 2632 m a.s.l. as detected by the monitoring data obtained by the Volcanic Observatory of Piton de la Fournaise (OVPF) (Roult et al., 2012). At 10:27 UTC a small and diluted gas plume was first visible and a vertical plume rapidly formed above the crater at 10:57 UTC. Up to 7 lava fountains erupted together from the same number of vents along a fracture on the west Dolomieu crater wall (length of fracture about 60 m) and the highest lava fountain of about 30 m was emitted by the largest vent located in the middle of the fracture. Lava flows were alimented by magma flowing from the vents (Fig. 1) but also from hot fountain products that were remobilized after falling down to the ground. According to Roult et al. (2012) the eruption emitted 1.2×10^6 m^3 of lava in about 9.6 days; mass flow rate decreased exponentially after the beginning of the eruption and the fountaining and gas plumes described here only occurred till 4 January 2010, whereafter mostly effusive lava flows were observed.

The vertical plume above the crater (Fig. 1; right) is relatively steady implying low winds and a level of neutral buoyancy is reached at approximately 1300 m above the fountain top (from observation). For the development of a parametrisation this case study is the least complex compared to other eruptions of PdF since 2000. There is a well-developed vertical gas column which is less impacted by the horizontal winds and the topography of the area.

2.2 Description of the volcanic plume parameterisation

It is well understood that a volcanic eruption plume enters into an atmosphere that has a pre-existing stratification, in terms of temperature, moisture content and wind (Bjornsson et al., 2011; Petersen et al., 2012). There are three dynamically distinct regions related to volcanic plumes (Sparks, 1986),

1. the gas thrust region, where the dynamics is dominated by the exit velocity at the vent and the flow near the vent is driven upward by its initial kinetic momentum,

2. buoyancy driven convective region which covers most of the height of the plume, and

GMDD
7, 8361–8397, 2014

3. umbrella cloud region where vertical motion is small and the plume disperses horizontally due to wind impacts.

For the purpose of modelling volcanic clouds using Méso-NH, we are predominately interested in the convective region of the volcanic cloud. The current updraft model used in Méso-NH defined by Pergaud et al. (2009), Sect. 2.2.1, is not adapted to volcanic clouds. In this section we propose an adaptation of the updraft scheme (Sects. 2.2.2 and 2.2.3) which is applied to volcanic plumes and consists mainly in a modification of the updraft initialization at ground level (z_{grd}) using values inspired from terrain observations.

2.2.1 Sub-grid cloud parameterisation as per Pergaud et al. (2009)

The basic idea of EDMF (Eddy Diffusivity Mass Flux) approach is to represent vertical transport of matter and energy that occur at the sub-grid scale in numerical simulations of convective boundary layer (CBL) with resolutions of ∼ 1 km or coarser. At such resolutions vertical motions usually dominate the vertical sub-grid transport due to

1. turbulent eddies
2. convective updrafts and compensating downdrafts.

Turbulent transport is commonly parameterised with the Eddy Diffusivity (ED) method, corresponding fluxes being written in the form of $-K_{\phi}\frac{\partial\overline{\phi}}{\partial z}$ where $-K_{\phi}$ is a diffusion coefficient and $\overline{\phi}$ the average of any model variable ϕ (e.g. temperature, tracer etc.) over the local grid cell (Holton, 2004).

A grid box can contain multiple convective updrafts, for simplicity a single updraft is considered carrying the properties of the ensemble of updrafts. This is known as the Mass-Flux (MF) approach. The fraction of the total area of a grid box that is covered by the updraft is known as the fractional updraft area (a_{u}). The corresponding net vertical

GMDD
7, 8361–8397, 2014

flux for ϕ over the grid cell takes the form of $\frac{M_u}{\rho}(\phi_u - \overline{\phi})$, where, M_u is the updraft mass flux, $\overline{\phi}$ is the mean value and ϕ_u is the updraft value of the variable ϕ.

Both ED and MF approaches have been combined in a single eddy diffusivity/mass flux (EDMF) parameterisation such that nonlocal sub-grid transport due to strong updrafts is taken into account by MF, while the remaining transport is taken into account by ED (Siebesma and Teixeira, 2000; Hourdin, 2002; Soares et al., 2004; Siebesma et al., 2007; Pergaud et al., 2009; Witek et al., 2011). In our approach for volcanic induced convection we only modify the MF scheme (Sect. 2.2.2).

The two key parameters determining the mass flux profile are entrainment (ε) and detrainment (δ) expressed as fractions of the updraft mass flux (M_u) per unit height. This simply leads to the following steady state mass flux continuity equation:

$$\frac{\partial M_u}{\partial z} = (\varepsilon - \delta) M_u \quad (1)$$

The mass-flux evolves along the vertical at a rate given by the difference between ε and δ rates. The definition of entrainment/detrainment rates is the crucial point in EDMF parameterisation as it is at this level that the physical coupling between turbulent mixing and mass flux is performed.

In Pergaud et al. (2009) the mass-flux profile depends on the vertical velocity of the updraft (w_u), whose vertical evolution is affected in turn by a buoyancy force (B_u) and a drag term where the entrainment of environmental air, namely lateral mixing, is accounted for:

$$w_u \frac{\partial w_u}{\partial z} = a\, B_u - b \varepsilon w_u^2 \quad (2)$$

The updraft buoyancy acceleration is evaluated related to the difference of virtual potential temperature (θ_v) between the updraft and its environment, in the absence of phase change in water: $B_u = g(\theta_{u,v} - \overline{\theta}_v)/\overline{\theta_v}$; parameters a and b are set to one (Simpson and Wiggert, 1969). Independent solutions of Eqs. (1) and (2) permit to calculate

GMDD
7, 8361–8397, 2014

the vertical variation of the updraft fractional area

$$a_u = \frac{M_u}{\rho w_u} \tag{3}$$

that is used to diagnose the cloud fraction, hence to define the sub-grid condensation scheme in the EDMF framework.

2.2.2 Modified EDMF – Updraft Initialisation

Firstly, in the current EDMF parameterisation w_u is initialised at the ground level (z_{grd}) using Turbulent Kinetic Energy (TKE) (e) as; $w_u^2(z_{grd}) = \frac{2}{3}e(z_{grd})$ which is bound to local meteorology. However, this computation is not applicable to volcanic plumes as vertical velocity in this case does not depend on the atmosphere, through the TKE. During volcanic eruptions, a mixture of gases, magma fragments, crystals and eroded rocks is injected into the atmosphere at high velocity, pressure and temperature. The diverse and unpredictable variability of eruptive styles depends mostly on the complex rheology of magma and the nonlinear processes leading to the fragmentation of the viscous melt into a mixture of gases and particles (Gonnermann and Manga, 2007). Nonetheless, the explosive character of a magmatic eruption like that of January 2010 is associated with the rapid decompression and the consequent abrupt expansion of gases in the magma (Parfitt and Wilson, 2008). In order to simplify, we consider the vertical velocity of the updraft $w_u(z_{grd})$ as the vertical velocity of the lava fountain (a variable that is mostly known from observation). The input data mentioned in this section (used for updraft initialisation) and the following sections are listed in Table 3.

Secondly, the updraft fraction area is simply initialised as the ratio of the fissure surface ($S_{Fis/SCM}$) by the model cell surface (S_{MNH}).

$$a_u(z_{grd}) = \frac{S_{Fis/SCM}}{S_{MNH}}. \tag{4}$$

GMDD
7, 8361–8397, 2014
Modelling of January 2010 Fournaise summit eruption using Méso-NH
S. G. Sivia et al.

Now, as $w_u(z_{grd})$ and $a_u(z_{grd})$ are both known and are independent of one another, using a similar principle as in Pergaud et al. (2009), the mass-flux at the ground can be calculated such that,

$$M_u(z_{grd}) = \rho_{mix}(z_{grd}) \times a_u(z_{grd}) \times w_u(z_{grd}), \quad (5)$$

where, the density of the updraft (approximated by a mixture of the two main gases at PdF; H_2O and SO_2) $\rho_{mix}(z_{grd}) = \frac{P(z_{grd})}{T_u(z_{grd}) r_{mix}}$. $P(z_{grd})$ is the pressure at ground level, $T_u(z_{grd})$ is the temperature of the updraft at ground level and r_{mix} represents the specific gas constant of the mixture. $r_{mix} = R(\frac{0.8}{M_{H_2O}} + \frac{0.2}{M_{SO_2}})$, where, R is the universal gas constant, M_{H_2O} is the molar mass of water vapour and M_{SO_2} is the molar mass of SO_2. In magmas like those erupted in 2010 the gas melange is dominated by water vapour, i.e. about 80 % of the melange (Di Muro et al., 2014), the remaining 20 % is that of SO_2 (i.e. $q_u = 0.8$ and $[SO_2] = 0.2\,\mathrm{kg\,kg^{-1}}$). This gives a $\frac{H_2O}{SO_2}$ ratio of 4, which is the ratio expected by simple closed system degassing of PdF shallow magmas. This values is at the lower end of the range actually measured by OVPF geochemical network (Allard et al., 2011). Hence, Eq. (5) uses ρ_{mix} rather than using density of dry/ambient air (in the standard formulation from Pergaud et al., 2009, Eq. 3).

2.2.3 Modified EDMF – Lateral mass exchange

Entrainment of ambient air through turbulent mixing plays a central role in the dynamics of eruption plumes, primarily because the plume density is controlled by the mixing ratio between ejected gas/material and ambient air (Suzuki and Koyaguchi, 2013). Furthermore the amount of air entrained controls the heights of eruption columns (Suzuki and Koyaguchi, 2010). In the current EDMF (Sect. 2.2.1), the mass flux entrainment of the updraft ε at the ground level is a constant value of $0.02\,\mathrm{m^{-1}}$ whereas δ is zero.

In this sub-section we present the modifications to the input method of ε and δ such that for some height above the ground (40 m), a desired mass of ambient air

GMDD
7, 8361–8397, 2014
Modelling of January 2010 Fournaise summit eruption using Méso-NH
S. G. Sivia et al.

may be entrained into the updraft and conversely, a desired mass of the updraft may be expelled. Above this height ε and δ are both calculated as defined by Pergaud et al. (2009) and the coexistence of entrainment/detrainment both continue to feed the vertical evolution of M_u.

The importance of adjusting the ground level ε and δ will become more apparent in Sect. 3 of results. However, due to the importance of this concept of entrainment and its associated effects on a volcanic column, the modifications are presented below. Figure 2 assembles all modifications made to EDMF model along with the input variables (marked in red) used at ground level.

Let M_{env} represent the mass flux of environmental air that enters the updraft between levels z_{grd} and $z_{grd} + \Delta z$. Hence updraft mass flux at $(z_{grd} + \Delta z)$ is simply defined as

$$M_u(z_{grd} + \Delta z) = M_u(z_{grd}) + M_{env}. \tag{6}$$

If $\alpha = \frac{M_{env}}{M_u(z_{grd}+\Delta z)}$ represents a fraction of environmental air in the melange at $z = z_{grd} + \Delta z$ then by rearranging Eq. (6),

$$\frac{M_u(z_{grd})}{M_u(z_{grd} + \Delta z)} = 1 - \alpha. \tag{7}$$

If ε and δ are constants between z_{grd} and $(z_{grd} + \Delta z)$ then by integrating Eq. (1) (Eq. (8) from Pergaud et al., 2009), between z_{grd} and $(z_{grd}+\Delta z)$, Eq. (7) can be rewritten as

$$\frac{M_u(z_{grd})}{M_u(z_{grd} + \Delta z)} = e^{-(\varepsilon-\delta)\Delta z}. \tag{8}$$

Finally using Eqs. (7) and (8)

$$1 - \alpha = e^{-(\varepsilon-\delta)\Delta z} \Leftrightarrow \varepsilon - \delta = -\frac{\ln(1-\alpha)}{\Delta z}. \tag{9}$$

For a desired fraction α of ambient air entrained in the volcanic gas column the entrainment and detrainment rates can be such that Eq. (9) is respected.

GMDD
7, 8361–8397, 2014

2.3 Simulation set-up and configuration

For our chosen case study three sets of simulations were run as depicted in Fig. 3.

1. Section 2.3.2 describes the 3-D spin-up simulation which is used to generate background atmospheric profiles.
2. Section 2.3.3 details the Large Eddy Simulation (LES) considered as the reference.
3. Section 2.3.4 outlines the 1-D single column model (SCM) simulation using the amended EDMF scheme as defined in Sect. 2.2.

Due to the computational efficiency of a 1-D model and the ability to isolate a column of atmosphere for study, SCM is an ideal environment in which to develop and test parameterisations (Randall et al., 1996). Observations relating to the case study are used to evaluate the LES simulations which are further used to validate the SCM results. This methodology has been used by the Global Energy and Water Cycle Experiment Cloud System Study (GCSS) (Browning, 1993) and EDMF scheme used to parameterise shallow convection (Pergaud et al., 2009). As outlined by Pergaud et al. (2009), both Siebesma et al. (2003) and Brown et al. (2002) have shown that LES are robust for representing shallow cumulus convection.

2.3.1 Common features to all simulations

Méso-NH model (version MNH-4-9-3) is used in this study, which is a mesoscale non-hydrostatic atmospheric model enabling it to simulate convective motion and flow over sharp topography. This model has been jointly developed by Laboratoire d'Aérologie (UMR 5560 UPS/CNRS) and Centre National de Recherches Météorologiques – Groupe d'études de l'Atmosphère Météorologique, CNRM-GAME (UMR 3589 CNRS/Météo-France) and is designed to simulate atmospheric circulations from small scale (type – LES) to synoptic scale phenomena (Lafore et al., 1998). All

GMDD
7, 8361–8397, 2014

Méso-NH related documentations and articles along with various model versions are available at http://mesonh.aero.obs-mip.fr.

Different sets of parameterisations have been introduced for cloud microphysics (Cohard and Pinty, 2000), turbulence (Bougeault and Lacarrere, 1989) and convection (Bechtold et al., 2001). The shallow convection in Méso-NH is parameterised according to Pergaud et al. (2009) while for the purposes of this study the deep convection option was deactivated. The ISBA (Interactions Soil-Biosphere–Atmosphere scheme) (Noilhan and Mafhaf, 1996) is the scheme used for land surfaces in order to parameterise exchanges between the atmosphere and the ground providing surface matter and energy fluxes to the atmosphere. The turbulent scheme implemented in Méso-NH is a full 3-D scheme that has been developed by Cuxart et al. (2000) with regards to both LES and mesoscale simulations. Kessler warm microphysical scheme (Kessler, 1969) was activated during the simulation. Méso-NH can be used for idealised as well as real case studies and for the purpose of this article we focus on idealised case studies. For all simulations performed a vertical grid composed of 72 levels in the Gal-Chen and Sommerville (1975) coordinate is used, with a vertical mesh stretched from 40 m at the ground to 600 m at the model top.

2.3.2 3-D spin-up simulation to generate background profiles

A three dimensional (3-D) spin-up simulation is performed to generate the background profiles which are used for SCM and LES. Two, two-way grid-nested domains with horizontal mesh sizes of 4 and 1 km are used (Fig. 3a). Both domains have 100 points in x and y. The initial state for the simulation, as well as the boundary conditions updated every six hours for the outermost model, are provided by analyses from the French Operations forecasting system for Indian Ocean, ALADIN-Reunion (9.6 km resolution; Montroty at al., 2008). The simulation starts 1 January 2010 at 00:00 UTC and ends 2 January 2010 at 18:00 UTC using a time step of 1 and 0.25 s for the 4 and 1 km resolution models respectively.

GMDD

7, 8361–8397, 2014

Figure 4 shows the vertical profiles of temperature (°C), potential temperature (K) and water vapour mixing ratio (g kg^{-1}) as simulated by the spin-up period for the local area of interest (location of the PdF volcano). The ambient atmosphere is dry with water vapour concentration just under $8\,\text{g kg}^{-1}$ at the ground and decreasing with altitude. The tropopause is found at about 16 km above ground level (a.g.l. hereafter, where the ground level corresponds to about 2.6 km a.s.l. – not shown) which corresponds well to tropical climates and the 0 °C isotherm is located at 2.7 km a.g.l.

The vertical structure of trade winds over Réunion Island was investigated by Lesouef (2010) and Lesouef et al. (2011). The trade wind inversion located at about 4 km a.s.l. (Taupin et al., 1999) is described as a consequence of the descending branch of the Hadley cell circulation (Lesouef et al., 2011) where easterly winds prevail in the lower levels while westerly winds prevail in upper levels. It coincides with a temperature inversion, or atleast a layer of enhanced vertical static stability. This is found in Fig. 4 (middle) at about 2 km a.g.l. (4.6 km a.s.l.) as an increased gradient of potential temperature. This stable layer can behave as a barrier for development of clouds (Hastenrath, 1991) and plumes generated through our simulations.

2.3.3 LES simulations

An LES model has such a high resolution that it can resolve not only convective motions but also the largest eddies (responsible for the majority of the turbulent transport). This section describes the initialisation of the LES simulation considered as reference used to validate the EDMF parameterisation for volcano induced convection.

The mass and heat fluxes values are prescribed for 1 LES cell (i.e. $S_{\text{Fis/LES}} = 100\,\text{m}^2$; Fig. 3c) with a correction factor (labelled Corr) of 1.2 such that the input fluxes are coherent with that of the SCM model, where $S_{\text{Fis/SCM}} = 120\,\text{m}^2$.

LES is initialised such that, for F_v representing the vapour mass flux ($\text{kg m}^{-2}\,\text{s}^{-1}$),

$$F_\text{v} = \rho_{\text{mix}} \times w_\text{u} \times q_\text{u} \times \text{Corr} \quad (10)$$

where ρ_{mix} is the density of the H_2O and SO_2 mixture in the updraft, where, $\rho_{mix} = \frac{P(z_{grd})}{T_u(z_{grd}) \times r_{mix}}$ and w_u is the vertical velocity of the updraft. Let F_s represent the sensible heat flux ($W\,m^{-2}$), then

$$F_s = T_u \times C_{p,\,mix} \times \rho_{mix} \times w_u \times \text{Corr} \quad (11)$$

where $C_{p,\,mix}$ is the specific heat capacity of the mixture (containing H_2O and SO_2) such that, $C_{p,\,mix} = 4r_{mix}$ and T_u is the temperature of the updraft. Finally, let F_{SO_2} represent the SO_2 mass flux ($kg\,m^{-2}\,s^{-1}$), then

$$F_{SO_2} = \rho_{mix} \times w_u \times [SO_2] \times \text{Corr}, \quad (12)$$

where $[SO_2]$ is the mixing ratio of SO_2 in the volcanic updraft. $S_{Fis/LES}$ the surface size of the LES grid cell of $100\,m^2$ and corrected by Corr = 1.2. Table 1 shows the configuration of the LES model.

To be noted that the wind profiles as obtained from the spin-up period have been stabilised i.e. $u = 0.1\,m\,s^{-1}$ and $v = 0\,m\,s^{-1}$ in LES (and for consistency also in SCM, Sect. 2.3.4). The reason for opting such a strategy is simply because a LES run with the wind fields extracted from the spin-up simulation shows a tilt in the volcanic plume (not shown) above the crater which is clearly not the case as observed in Fig. 1, implying that the wind fields do not appear to be realistic. The average wind speed (10 m above the caldera rim of Bellecombe) provided by Météo France is of $2.3 \pm 1.5\,m\,s^{-1}$ for the period 2–11 January. Due to the short simulation duration, radiative processes are neglected (i.e. the downward radiative flux is put to zero) and orography of the region is not taken into account, depicting a flat domain for simplifying the model (as also done for SCM model detailed in Sect. 2.3.4).

2.3.4 SCM simulation

Table 2 shows the configuration of SCM model. The volcanic updraft is simulated only in a single central grid cell of size 1 km × 1 km, however the total number of grid cells

Discussion Paper | Discussion Paper | Discussion Paper | Discussion Paper |

GMDD

7, 8361–8397, 2014

Modelling of January 2010 Fournaise summit eruption using Méso-NH

S. G. Sivia et al.

used are 3 × 3 (Fig. 3b). This is simply to allow for the use of open lateral boundary conditions, and hence avoid matter and energy to accumulate in the model. As for the LES (Sect. 2.3.3) the wind profiles obtained from the spin-up period and used as background conditions have been stabilised. The LES simulation is compared to central SCM grid cell of 1 km × 1 km as sketched in Fig. 3.

The adapted EDMF model in Sect. 2.2.2 is used to run this simulation and the variables used to initialise the model are detailed in Table 3 for both SCM and LES, along with their respective formulae (where necessary) and values. As mentioned earlier, since the gas melange in the eruption column consists of 80 % of H_2O and 20 % of SO_2, the SCM model is simply initialised with $q_u = 0.8\,\mathrm{kg\,kg^{-1}}$ and $[SO_2] = 0.2\,\mathrm{kg\,kg^{-1}}$ in the updraft at ground level. As for the LES, due to the short simulation duration radiative processes are neglected.

3 Results and analysis

In this section results obtained from the 1-D SCM and 3-D LES of the case study are presented and analysed.

3.1 Need of specific heat source to generate deep plumes

A first most obvious question is whether we need to parameterise volcanic updraft? Figure 5 shows results from 4 simulations; Fig. 5a and b shows simulation results for LES model without and with volcanic heat sources respectively, whereas Fig. 5c and d show results from the 1-D SCM model without and with volcanic heat source respectively. Results for Fig. 5b follow the initialisation of volcanic heat source as outlined in Sect. 2.3.3 above and results from Fig. 5d follow the initialisation of volcanic heat source as outlined in Sect. 2.2.2. All four simulations have been initialised with a passive SO_2 tracer as outlined in Table 3 and used as a tracer pollutant injected into the atmosphere. The vertical profiles of SO_2 tracer depicted are horizontally averaged over

GMDD
7, 8361–8397, 2014

the 1 km × 1 km domain for LES simulations (Fig. 5a and c), whereas, for the SCM they are the outputs of the central 1 km × 1 km grid (Fig. 5b and d) as depicted in Fig. 3.

In simulations with no volcanic heat source, SO_2 tracer is simply diffused to a few hundreds of meters above the ground and majority of the tracer remains at low altitude (Fig. 5a and c). Results from the reference LES simulation (Fig. 5b) shows an uplift of tracer to higher altitudes, with maximum concentration levelled off at around 1.2–1.4 km and a vertical distribution up to 3.75 km above the ground. Similarly, the SCM simulation with modified EDMF (M.EDMF) results (Fig. 5d) also shows tracer lifted to much higher altitudes with majority of the concentration levelled at around 7.25 km. The overall tracer concentrations are vertically distributed between 4 and 11 km above the ground. It is clear that without modifications to EDMF and without initialising LES simulation with volcanic heat sources, the two models are not capable to transport tracer concentrations to higher altitudes.

Although at this stage both Fig. 5b and d show a successful transport of tracer to higher altitudes, it is evident that in terms of maximum detrainment height of the tracer (1.4 and 7.25 km respectively) and its vertical profile, the M.EDMF results are not comparable to that of the LES (the reference simulation); plume generated by M.EDMF is too deep. Hereafter, the height at which there is a maximum detrainment of the tracer will be referred to as the "maximum injection height".

3.2 Influence of entrainment/detrainment at the base of the updraft

It is well known that both entrainment and detrainment have an impact on the updraft development because they affect buoyancy (Woods, 1988; Glaze et al., 1997; Graf et al., 1999; Kaminski et al., 2005; Carazzo et al., 2008) at all updraft levels.

Figure 6 shows the updraft temperature profile for the plume generated in Fig. 5d (left) and the temperature of the plume taken through Infrared (IR) imagery for the PdF eruption of October 2010 (right, as no IR imagery is available for January 2010). The IR imagery shows a temperature of approximately ranging between 55–60 °C (labelled Pnt1 on Fig. 6, right and the temperature labelled Z2Mx is the average temperature of

GMDD
7, 8361–8397, 2014

the box labelled Z2) for the buoyant region of the plume which is comparable to the upper bound of the first model level, at $\Delta z = 40$ m a.g.l. The comparison is very crude and qualitative but at least, it shows that the updraft temperature at the base of our simulated plume of Fig. 5d is not in a correct range of temperatures and consequently the plume is too buoyant and too deep, as not enough fresh ambient air is entrained in the plume base. To correct this discrepancy there is a need to modify the entrainment and detrainment rates at the base of M.EDMF model (as described in Sect. 2.2.3).

The sensitivity of our model to various percentages of ambient air entrained into the updraft at one Δz above the ground is shown in Fig. 7.

Here, briefly the labels 1E, 2E and 3E used in Fig. 7 are explained. Using Eq. (9) where, $\varepsilon - \delta = -\frac{\ln(1-\alpha)}{\Delta z}$, for a given value of α (percentage of ambient air entrained into the volcanic gas column), let $\varepsilon(\alpha) = -\frac{\ln(1-\alpha)}{\Delta z}$. Therefore, we define 1E to correspond to $\varepsilon = \varepsilon(\alpha)$ and $\delta = 0$, 2E to correspond to $\varepsilon = 2\varepsilon(\alpha)$ and $\delta = \varepsilon(\alpha)$, and finally 3E corresponds to $\varepsilon = 3\varepsilon(\alpha)$ and $\delta = 2\varepsilon(\alpha)$.

The M.EDMF model is very sensitive to entrainment and detrainment rates (Fig. 7). Entraining low percentages of ambient air into the updraft aids the plume to reach higher altitudes and conversely higher percentages of entrainment leads to a lower heights. This is due to the dilution of the updrafts which decreases the density of the plume as the ambient atmosphere is much drier (Fig. 4) and cooler with respect to the hotter plume. This also dilutes the water vapour contained within the plume hence affecting the release of latent heat within the plume. From Fig. 7 it is clear that to decrease the injection height of M.EDMF plume (Fig. 5d) such that it is comparable to the LES result (Fig. 5b), an infinite range of possibilities exist for modifications of entrainment/detrainment at the first model level, e.g. modifications related to 1E, 2E and 3E etc.

Figure 8 shows the simulation results for SO_2 tracer whereby the α values are tuned in M.EDMF (Sect. 2.2.3) such that the injection height matches the LES results for each of the 1E, 2E and 3E cases.

GMDD
7, 8361–8397, 2014
Modelling of January 2010 Fournaise summit eruption using Méso-NH
S. G. Sivia et al.

Title Page
Abstract Introduction
Conclusions References
Tables Figures
◂◂ ▸▸
◂ ▸
Back Close
Full Screen / Esc
Printer-friendly Version
Interactive Discussion

Although the injection height for three cases in Fig. 8 are comparable to that of LES, the tracer concentrations are more diluted as the magnitude of entrainment and detrainment is increased (Fig. 8b and c compared to Fig. 8a). The most fitted SO_2 concentration with LES (from the three cases explored) is that obtained in Fig. 8a for $\alpha = 0.834$ and an ε/δ distribution of type 1E (i.e. no detrainment; $\delta = 0$) after 90 min of simulation time. The vertical distribution of the tracer is also satisfactory with that obtained from LES, although M.EDMF does overestimate the concentrations at altitudes below 1 km and above 1.6 km. Globally, the results obtained are satisfactory and through this sub-grid parameterisation the SO_2 tracer has been injected correctly into higher altitudes.

SO_2 concentrations have served to adjust the parameterisation parameters (α, ε and δ) with the best tuning ($\alpha = 0.834$, case 1E) which is used from now on.

Figure 9a shows the maximum detrainment observed at about 1–1.4 km a.g.l. which coincides with the maximum detrainment of the tracer at the same level Fig. 8a. The entrainment and detrainment both reach zero at around 6 km a.g.l. indicating the maximum height of the updraft and once again SCM tracer concentrations reach zero at this height (Fig. 8a). Note also that detrainment is weak below 0.75 km.

Figure 9b also shows the anomalies of water vapour mixing ratio (q_u) for LES and M.EDMF model, i.e. $q_u(t_{90}) - q_u(t_0)$, where t_0 and t_{90} is simulation time of 0 min and 90 min respectively. Although at near ground level the M.EDMF shows lower water vapour concentration at t_{90} than the LES model (due to the modification in entrainment at ground level), in higher altitudes (≥ 0.5 km) the two models are in fairly good agreement.

4 Conclusions

In order to represent deep convective injections of volcanic emissions into the low to mid troposphere in case of effusive eruptions, the EDMF parameterisation by Pergaud et al. (2009) has been adapted. The adapted EDMF scheme takes into account the intense and localised input of sensible and latent heat near eruptive vent and induces a sub-grid convective plume.

We have shown the need to input specific heat source in order to generate deep plumes using the Méso-NH model by adapting the EDMF scheme. LES simulation were also initialised using water vapour mass flux, sensible heat flux and SO_2 mass flux for the same area as for the M.EDMF model. In absence of appropriate terrain observations, the LES simulation (considered as a reference) was used to validate the EDMF parameterisation for volcano induced convection (i.e. M.EDMF model). LES and M.EDMF model have both been successful in generating deep plumes and hence transporting SO_2 tracer to higher altitudes. We have further demonstrated the need to modify the existing lateral mass exchanges a few tens of meters above the localised heat source in SCM model as without this modification the plumes generated are too deep because of overestimated temperatures few tens of meters above the ground. The sensitivity of our model to lateral mass exchanges at 40 m above the ground (first model level above the ground) have been presented while further aiding us to tune our model (for SO_2 tracer concentrations) such that SCM results are coherent with the results obtained from LES.

Entrainment of ambient air in a volcanic plume is largely known to be one of the key parameters affecting it's buoyancy. Since the first experiments by Morton et al. (1956), extensive research (modelling studies or laboratory experiments) has been deployed to constrain this sensitive parameter (e.g. Wright, 1984; Hunt and Kaye, 2001; Kaminski et al., 2005; Carazzo et al., 2008). Although, great advancements have been made by differentiating between the different regimes; volcanic jets, strong plumes and collapsing columns, it is clear from the comprehensive review found in Tate (2002) and Matulka et al. (2014) that this is still an area of open research. For our case SO_2 concentrations have served to adjust the parameterisation parameters (α, ε and δ) with the best tuning and furthermore impact of the volcanic plume on the humidity profile by further comparing LES and SCM results, showing a good agreement. The best fit was

GMDD
7, 8361–8397, 2014

obtained with a large fraction of fresh air incorporated into the plume (α = 83.4 %) and no detrainment.

Although this parameterisation has been used in an idealised and controlled set-up for one particular case study (January 2010 summit eruption) further work needs to be undertaken whereby, the parameterisation needs to be tested for different eruptions (i.e. changes in volcanic heat sources, idealised and real case simulations). Furthermore, the tuning of entrainment and detrainment needs to be further investigated such that it too is tested for different eruptions cases and ideally a single tuning factor which may be applied to various eruption cases.

Code availability

Meso-NH model documentation and the model itself is available from the website mesonh.aero.obs-mip.fr. A licence is required to acquire the model version 4-9-3 with the supporting documentation available from the website. The specific routines needed for the purpose of this research paper will then be made available in order to reproduce the results. The licence can be acquired by contacting the Meso-NH team's scientific coordinator, Jean-Pierre Chaboureau (jean-pierre.chaboureau@aero.obs-mip.fr), whereas the specific routines will be supplied by the corresponding author F. Gheusi (francois.gheusi@aero.obs-mip.fr).

Acknowledgements. We greatly acknowledge Observatoire Volcaniques de Piton de la Fournaise – OVPF for providing the pictures of the January 2010 summit eruption along with information relating to the eruption itself. We also thank the Méso-NH assistance team for continuous support and C. Barthe and Meteo-France for kindly providing us with ALADIN-REUNION atmospheric files. This work was performed using HPC resources from GENCI-IDRIS (Grantx2014010005) and CALMIP (Grant P12171). We wish to acknowledge the use of the NCAR Command Language (NCL, Boulder, Colorado) version 6.0.0 software for analysis and graphics in this paper. And finally, we thank the Observatoire des Milieux Naturels et des Changements globaux (OMNCG) and Observatoires des Sciences de l'Univers (OSU), Réunion along with the MoPAV project of the LEFE – CHAT program by INSU – CNRS (Institut

GMDD
7, 8361–8397, 2014

National des Sciences de l'Univers of Centre National de la Recherche Scientifique) for their financial support and interest in this project.

References

Allard, P., La Spina, A., Tamburello, G., Aiuppa, A., Burton, M., Di Muro, A., and Staudacher, T.: First measurements of magmatic gas composition and fluxes during an eruption (October 2010) of Piton de la Fournaise hot spot volcano, La Reunion island, Geophysical Research Abstracts, Vol. 13, 2011 EGU, GMPV-5, Oral Presentation, 2011. 8369

Bechtold, P., Bazile, E., Guichard, F., Mascart, P., and Richard, E.: A mass-flux convection scheme for regional and global models, Q. J. Roy. Meteor. Soc., 127, 869–886, 2001. 8372

Bjornsson, H., Magnusson, S., Arason, P., and Petersen, G. N.: Assessing simple models of volcanic plumes using observations from the summit eruption of Eyjafjallajökull in 2010, American Geophysical Union, Fall Meeting, San Francisco, 2011. 8365

Bhugwant, C., Sieja, B., Bessafi, M., Staudacher, T., and Ecormier, J.: Atmospheric sulfur dioxide measurements during the 2005 and 2007 eruptions of the Piton de La Fournaise volcano: implications for human health and environmental changes, J. Volcanol. Geoth. Res., 184, 208–224, doi:10.1016/j.jvolgeores.2009.04.012, 2009. 8363

Bougeault, P. and Lacarrere, P.: Parametrization of orography-induced turbulence in a mesobeta model, Mon. Weather Rev., 117, 1872–1890, 1989. 8372

Brown, A., Cederwall, R. T., Chlond, A., Duynkerke, P. G., Golaz, J. C., Khairoutdinov, M., Lewellen, D., Lock, A. P., Macvean, M. K., Moeng, C. H., Neggers, R. A. J., Siebesma, P., and Stevens, B.: Large-eddy simulation of the diurnal cycle of shallow cumulus convection over land, Q. J. Roy. Meteor. Soc., 128, 1075–1093, 2002. 8371

Browning, K. A.: The GEWEX Cloud System Study (GCSS), B. Am. Meteorol. Soc., 74, 387–399, 1993. 8371

Bursik, M.: Effect of wind on the rise height of volcanic plumes, Geophys. Res. Lett., 28, 3621–3624, 2001. 8362

Carazzo, G., Kaminski, E., and Tait, S.: On the rise of turbulent plumes: quantitative effects of variable entrainment for submarine hydrothermal vents, terrestrial and extra terrestrial explosive volcanism, J. Geophys. Res., 113, B09201, doi:10.1029/2007JB005458, 2008. 8376, 8379

GMDD

7, 8361–8397, 2014

Modelling of January 2010 Fournaise summit eruption using Méso-NH

S. G. Sivia et al.

Cohard, J. and Pinty, J.: A comprehensive two-moment warm microphysical bulk scheme, II: 2D experiments with a non hydrostatic model, Q. J. Roy. Meteor. Soc., 126, 1843–1859, 2000. 8372
Cuxart, J., Bougeault, P., and Redelsperger, J. L.: A turbulence scheme allowing for mesoscale and large-eddy simulations. Q. J. Roy. Meteor. Soc., 126, 1–30, 2000. 8372
Delmelle, P., Stix, J., Baxter, P., Garcia-Alvarez, J., and Barquero, J.: Atmospheric dispersion, environmental effects and potential health hazard associated with the low-altitude gas plume of Masaya volcano, Nicaragua, B. Volcanol., 64, 423–434, 2002. 8363
Di Muro, A., Staudacher, T., Ferrazzini, V., Villemant, B., Besson, P., and Garofalo, C.: Tracking Magma Injection in the Piton de la Fournaise Volcanic Edifice after the 2007 Summit Caldera Collapse by Pele's Hair Composition, Chapman Special Volume on Hawaiian volcanoes, AGU Books, 2014. 8369
Gal-Chen, T. and Somerville, R. C. J.: On the use of a coordinate transformation for the solution of the Navier–Stokes equations, J. Comput. Phys., 17, 209–228, doi:10.1016/0021-9991(75)90037-6, 1975. 8372
Glaze, L. S. and Baloga, S. M.: Sensitivity of buoyant plume heights to ambient atmospheric conditions: implications for volcanic eruption columns, J. Geophys. Res., 101, 1529–1540, 1996. 8362
Glaze, L. S., Baloga, S. M., and Wilson, L.: Transport of atmospheric water vapor by volcanic eruption columns, J. Geophys. Res., 102, 6099–6108, 1997. 8376
Gonnermann, H. M. and Manga, M.: The fluid mechanics inside a volcano, Annu. Rev. Fluid Mech., 39, 321–356, 2007. 8368
Graf, H., Herzog, M., Oberhuber, J. M., and Textor, C.: Effect of environmental conditions on volcanic plume rise, J. Geophys. Res., 104, 24309–24320, 1999. 8362, 8376
Hastenrath, S.: Climate Dynamics of the Tropics, Kluwer Academy, 1991. 8373
Herzog, M., Oberhuber, J. M., and Graf, H.: A prognostic turbulence scheme for the non-hydrostatic plume model ATHAM, J. Atmos. Sci., 60, 2783–2796, 2003.
Holton, J. R.: An Introduction to Dynamic Meteorology, Elsevier Academic Press, 2004. 8366
Hourdin, F., Couvreux, F., and Menut, L.: Parameterization of the dry convective boundary layer based on a mass flux representation of thermals, J. Atmos. Sci., 59, 1105–1123, 2002. 8367
Hunt, G. R. and Kaye, N. G.: Virtual origin correction for lazy turbulent plumes, J. Fluid Mech., 435, 377–396, 2001. 8379

GMDD
7, 8361–8397, 2014

Kaminski, E., Tait, S., and Carazzo, G.: Turbulent entrainment in jets with arbitrary buoyancy, J. Fluid Mech., 526, 361–376, 2005. 8376, 8379

Kessler, E.: On the distribution and continuity of water sustance in atmospheric circulations, Meteor. Monogr., 10, 1–84, 1969. 8372

Lafore, J. P., Stein, J., Asencio, N., Bougeault, P., Ducrocq, V., Duron, J., Fischer, C., Héreil, P., Mascart, P., Masson, V., Pinty, J. P., Redelsperger, J. L., Richard, E., and Vilà-Guerau de Arellano, J.: The Meso-NH Atmospheric Simulation System. Part I: adiabatic formulation and control simulations, Ann. Geophys., 16, 90–109, doi:10.1007/s00585-997-0090-6, 1998. 8363, 8371

Lenat, J. and Bachelery, P.: Dynamics of magma transfer at Piton de La Fournaise Volcano (Reunion Island, Indian Ocean), in: Earth Evolution Sciences – Special Issue Modeling of Volcanic Processes, edited by: Chi-Yu, K. and Scarpa, R., Friedr. Vieweg and Sohn, Brauschweig/Wiesbaden, 57–72, 1987. 8363

Lesouëf, D.: Numerical studies of local atmospheric circulations over Reunion island: application to the dispersion of pollutants, Ph. D. thesis, available at: http://tel.archives-ouvertes.fr/tel-00633096 (last access: 14 February 2014), 2010. 8373

Lesouëf, D., Gheusi, F., Delmas, R., and Escobar, J.: Numerical simulations of local circulations and pollution transport over Reunion Island, Ann. Geophys., 29, 53–69, doi:10.5194/angeo-29-53-2011, 2011. 8363, 8373

Mather, T. A., Pyle, D. M., and Oppenheimer, C.: Tropospheric volcanic aerosol, in: Volcanism and the Earth's Atmosphere, American Geophysical Union, 189–212, doi:10.1029/139GM12, 2003. 8363

Matulka, A., López, P., Redondo, J. M., and Tarquis, A.: On the entrainment coefficient in a forced plume: quantitative effects of source parameters, Nonlin. Processes Geophys., 21, 269–278, doi:10.5194/npg-21-269-2014, 2014. 8379

Morton, B. R., Taylor, G., and Turner, J. S.: Turbulent gravitational convection from maintained and instantaneous sources, P. Roy. Soc. Lond. A Mat., 234, 1–23, doi:10.1098/rspa.1956.0011, 1956. 8379

Montroty, R., Rabier, F., Westrelin, S., Faure, G., and Viltard, N.: Impact of wind bogus and cloud- and rain- affected SSM/I data on tropical cyclone analyses and forecasts, Q. J. Roy. Meteor. Soc., 134, 1673–1699, 2008. 8372

Noilhan, J. and Mahfouf, J. F.: The ISBA land surface parameterization scheme, Global Planet. Change, 13, 145–159, 1996. 8372

GMDD
7, 8361–8397, 2014

Modelling of January 2010 Fournaise summit eruption using Méso-NH

S. G. Sivia et al.

Parfitt, E. A. and Wilson, L.: Fundamentals of Physical Volcanology, Blackwell Publishing, Malden, USA, 2008. 8368

Peltier, A., Staudacher, T., Bachelery, P., and Cayol, V.: Formation of the April 2007 caldera collapse at Piton de La Fournaise volcano: insights from GPS data, J. Volcanol. Geoth. Res., 184, 152–163, doi:10.1016/j.jvolgeores.2008.09.009, 2009. 8363

Pergaud, J., Masson, V., Malardel, S., and Couvreux, F.: A parameterization of dry thermals and shallow cumuli for mesoscale numerical weather prediction, Bound.-Lay. Meteorol., 132, 83–106, 2009. 8362, 8364, 8366, 8367, 8369, 8370, 8371, 8372, 8378

Petersen, G. N., Bjornsson, H., and Arason, P.: The impact of the atmosphere on the Eyjafjallajökull 2010 eruption plume, J. Geophys. Res., 117, D00U07, doi:10.1029/2011JD016762, 2012. 8365

Randall, D. A., Albrecht, B., Cox, S., Johnson, D., Minnis, P., Rossow, W., and Starr, D. O.: On fire at ten, Adv. Geophys., 38, 37–128, 1996. 8371

Robock, A.: Volcanic eruptions and climate, Rev. Geophys., 38, 191–219, doi:10.1029/1998RG000054, 2000. 8363

Roult, G., Peltier, A., Taisne, B., Staudacher, T., Ferrazzini, V., Di Muro, A., and the OVPF team: A new comprehensive classi fication of the Piton de la Fournaise activity spanning the 1985–2010 period. Search and analysis of short-term precursors from a broad-band seismological station, J. Volcano. Geoth. Res., 241–242, 78–104, 2012. 8365

Siebesma, A. P. and Teixeira, J.: An advection–diffusion scheme for the convective boundary layer: description and 1d-results, in: Proc. 14th Symposium on Boundary Layers and Turbulence, Amer. Met. Soc., Aspen, CO, USA, 7–11 August, 133–136, 2000. 8367

Siebesma, P., Bretherton, C. S., Brown, A., Chlond, A., Cuxart, J., Duynkerke, P. G., Jiang, H., Khairoutdinov, M., Lewellen, D., Moeng, C. H., Sanchez, E., Stevens, B., and Stevens, D. E.: A large eddy simulation intercomparison study of shallow cumulus convection, J. Atmos. Sci., 60, 1201–1219, 2003. 8371

Siebesma, P., Soares, P. M. M., and Teixeira, J.: A combined eddy-diffusivity mass-flux approach for the convective boundary layer, J. Atmos. Sci., 64, 1230–1248, 2007. 8367

Simpson, J. and Wiggert, V.: Models of precipitating cumulus towers, Mon. Weather Rev., 97, 471–489, 1969. 8367

Soares, P. M. M., Miranda, P. M. A., Siebesma, A. P., and Teixeira, J.: An eddy-diffusivity/mass-flux parameterization for dry and shallow cumulus convection, Q. J. Roy. Meteor. Soc., 130, 3055–3079, 2004. 8367

GMDD
7, 8361–8397, 2014

Modelling of January 2010 Fournaise summit eruption using Méso-NH

S. G. Sivia et al.

Sparks, R. S. J.: The dimensions and dynamics of volcanic eruption columns, B. Volcanol., 48, 3–15, 1986. 8365

Strada, S., Mari, C., Filippi, J. B., and Bosseur, F.: Wildfire and the atmosphere: modelling the chemical and dynamic interactions at the regional scale, Atmos. Environ., 51, 234–249, doi:10.1016/j.atmosenv.2012.01.023, 2012. 8363

Suzuki, Y. J. and Koyaguchi, T.: Numerical determination of the efficiency of entrainment in volcanic eruption columns, Geophys. Res. Lett., 37, L05302, doi:10.1029/2009GL042159, 2010. 8369

Suzuki, Y. J. and Koyaguchi, T.: 3D numerical simulation of volcanic eruption clouds during the 2011 Shinmoe-dake eruptions, Earth Planets Space, 65, 581–589, 2013. 8369

Tate, P. M.: The rise and dilution of buoyant jets and their behaviour in an internal wave field, Ph. D. thesis, University of New South Wales, available at: http://books.google.fr/books?id=1Aw3NQAACAAJ (last access: 16 September 2014), 2002. 8379

Taupin, F. G., Bessafi, M., Baldy, S., and Bremaud, P. J.: Tropospheric ozone above the south-western Indian Ocean is strongly linked to dynamical conditions prevailing in the tropics, J. Geophys. Res., 104, 8057–8066, 1999. 8373

Tulet, P. and Villeneuve, N.: Large scale modeling of the transport, chemical transformation and mass budget of the sulfur emitted during the April 2007 eruption of Piton de la Fournaise, Atmos. Chem. Phys., 11, 4533–4546, doi:10.5194/acp-11-4533-2011, 2011. 8363

Tupper, A., Textor, C., Herzog, M., Graf, H. F., and Richards, M. S.: Tall clouds from small eruptions: the sensitivity of eruption height and fine ash content to tropospheric instability, Nat. Hazards, 51, 375–401, doi:10.1007/s11069-009-9433-9, 2009. 8362

Viane, C., Bhugwant, C., Sieja, B., Staudacher, T., and Demoly, P.: Etude comparative des emissions de gaz volcanique du Piton de la Fournaise et des hospitalisations pour asthme de la population reunionnaise de 2005 a 2007, Rev. Fr. Allergol., 49, 346–357, 2009. 8363

Witek, M. L., Teixeira, J., and Matheou, G.: An eddy-diffusivity/mass-flux approach to the vertical transport of turbulent kinetic energy in convective boundary layers, J. Atmos. Sci., 68, 2385–2394, doi:10.1175/JAS-D-11-06.1, 2011. 8367

Woods, A. W.: The fluid dynamics and thermodynamics of eruption columns, B. Volcanol., 50, 169–193, 1988. 8376

Wright, S.: Buoyant jets in density-stratified cross flow, J. Hydraul. Eng-ASCE, 110, 643–656, 1985. 8379

GMDD
7, 8361–8397, 2014

Modelling of January 2010 Fournaise summit eruption using Méso-NH

S. G. Sivia et al.

Title Page
Abstract | Introduction
Conclusions | References
Tables | Figures
◀| |▶
◀ ▶
Back | Close
Full Screen / Esc
Printer-friendly Version
Interactive Discussion

Table 1. LES model configuration.

Configuration	LES
Δx, Δy (m)	10
Δt (s)	0.01
No. of points in $x \times y$	100 × 100
Total run (min)	90
Start time (UTC)	10:50

GMDD
7, 8361–8397, 2014

Table 2. SCM model configuration.

Configuration	SCM
Δx, Δy (m)	1000
Δt (s)	1
No. of points in $x \times y$	3×3
Total run (min)	90
Start time (UTC)	10:50

GMDD
7, 8361–8397, 2014

Table 3. Variables and values used for LES and SCM models.

Variable	Notation	Model	Formula	Value	Units	Data type
Updraft H_2O mixing ratio	q_u	SCM/LES	n/a	0.8	$kg\,kg^{-1}$	Input
Updraft SO_2 mixing ratio	$[SO_2]$	SCM/LES	n/a	0.2	$kg\,kg^{-1}$	Input
H_2O by SO_2 ratio	$\frac{H_2O}{SO_2}$	SCM/LES	$\frac{q_u}{[SO_2]}$	4	n/a	n/a
Updraft vertical velocity	w_u	SCM/LES	n/a	24	$m\,s^{-1}$	Input
Updraft temperature at ground	$T_u(z_{grd})$	SCM/LES	n/a	1320	K	Input
Pressure at ground	$P(z_{grd})$	SCM/LES	n/a	78 695	Pa	Input
Universal gas constant	R	SCM/LES	n/a	8.314	$J\,mol^{-1}\,K^{-1}$	Constant
Molar mass of H_2O	M_{H_2O}	SCM/LES	n/a	0.018	$kg\,mol^{-1}$	Constant
Molar mass of SO_2	M_{SO_2}	SCM/LES	n/a	0.064	$kg\,mol^{-1}$	Constant
Specific gas constant of the mixture (H_2O and SO_2)	r_{mix}	SCM/LES	$R(\frac{0.8}{M_{H_2O}} + \frac{0.2}{M_{SO_2}})$	395.49	$J\,kg^{-1}\,K^{-1}$	n/a
Density of the mixture at ground	$\rho_{mix}(z_{grd})$	SCM/LES	$\frac{P(z_{grd})}{T_u(z_{grd}) \times r_{mix}}$	0.15	$kg\,m^{-3}$	n/a
Area of the fissure	$S_{Fis/SCM}$	SCM	n/a	120	m^2	Input
Area of Meso-NH cell	S_{MNH}	SCM	$\Delta x \times \Delta y$	1×10^6	m^2	Input
Updraft area	a_u	SCM	$\frac{S_{Fis/SCM}}{S_{MNH}}$	1.2×10^{-4}	n/a	Input
Ratio of ambient air entrained	α	SCM	n/a	0.834	n/a	Input
Area of the fissure	$S_{Fis/LES}$	LES	n/a	100	m^2	Input
Correction factor	Corr	LES	$\frac{S_{Fis/SCM}}{S_{Fis/LES}}$	1.2	n/a	n/a
Specific gas constant of the mixture	$C_{p,\,mix}$	LES	$4r_{mix}$	1581.96	$J\,kg^{-1}\,K^{-1}$	n/a
H_2O mass flux	F_v	LES	$\rho_{mix} \times w_u \times q_u \times Corr$	3.456	$kg\,m^{-2}\,s^{-1}$	Input
Sensible heat flux	F_s	LES	$T_u \times C_{p,\,mix} \times \rho_{mix} \times w_u \times Corr$	9×10^6	$W\,m^{-2}$	Input
SO_2 mass flux	F_{SO_2}	LES	$\rho_{mix} \times w_u \times [SO_2] \times Corr$	0.864	$kg\,m^{-2}\,s^{-1}$	Input

GMDD
7, 8361–8397, 2014

Modelling of January 2010 Fournaise summit eruption using Méso-NH

S. G. Sivia et al.

Figure 1. January 2010 summit eruption of Piton de la Fournaise: the 60 m long fissure on the cliff of Dolomieu summit crater emits lava flows towards the bottom of the caldera. The < 30 m high fountains (left) are the source of the ca. 1 km high vertical plume (right) of gas and vapour. Transport and sedimentation of solid particles are mostly confined to the lowest portion (< 100 m) of the plume. Pictures provided by the Piton de la Fournaise Volcanological Observatory (OVPF/IPGP).

GMDD
7, 8361–8397, 2014

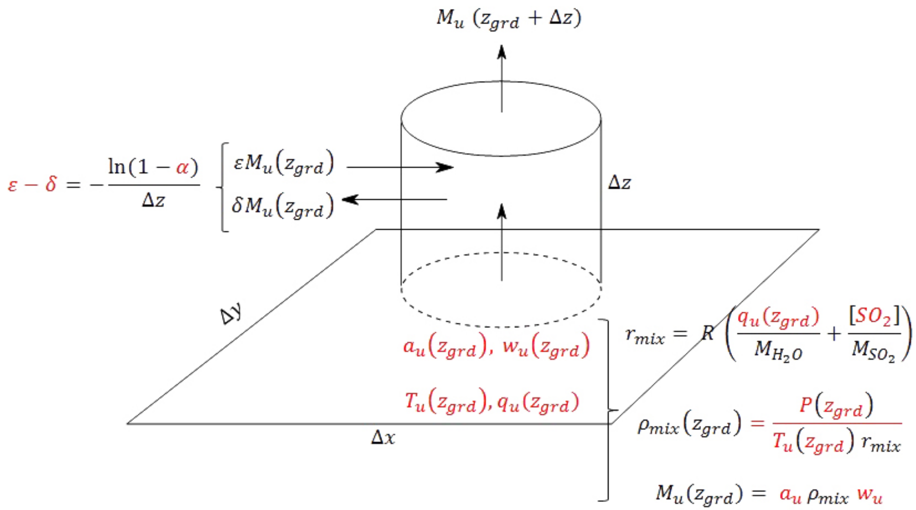

Figure 2. Figure displaying the input data the mass flux at ground level (z_{grd}) and the mass flux at level $z_{grd}+\Delta z$ after the incorporation of environmental air mass. The input variables of the model are highlighted in red.

GMDD
7, 8361–8397, 2014
Modelling of January 2010 Fournaise summit eruption using Méso-NH
S. G. Sivia et al.

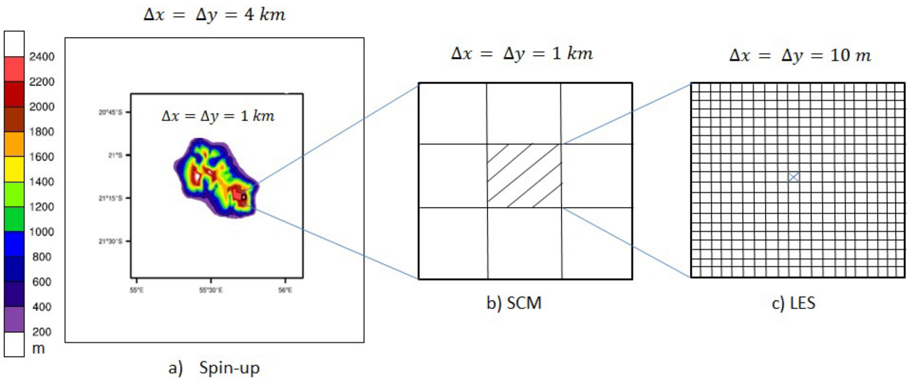

Figure 3. The interconnection in terms of the simulation domain between the three sets of simulations performed, namely; Spin-up, SCM and LES. The one cell corresponding to the fissure is tagged for LES.

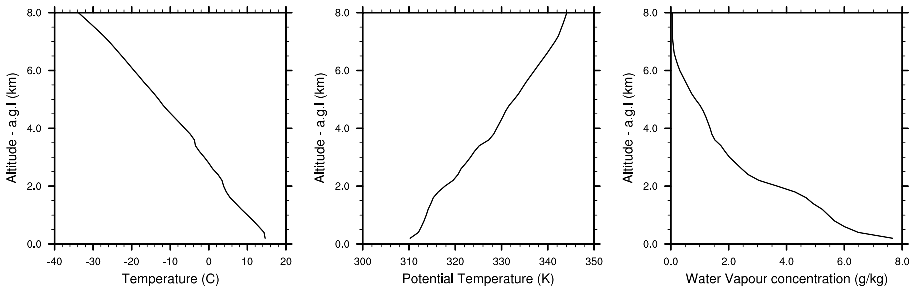

Figure 4. Meteorological profiles from the spin-up model (1 km resolution) at the location of the January 2010 summit eruption on 2 January 2010 at 10:50 UTC. Vertical profiles of temperature (°C), potential temperature (K) and water vapour mixing ratio at the grid scale ($g\,kg^{-1}$). Altitude displayed is above ground level (a.g.l.), i.e. 2600 m a.s.l.

GMDD
7, 8361–8397, 2014
Modelling of January 2010 Fournaise summit eruption using Méso-NH
S. G. Sivia et al.

Title Page
Abstract | Introduction
Conclusions | References
Tables | Figures
Back | Close
Full Screen / Esc
Printer-friendly Version
Interactive Discussion

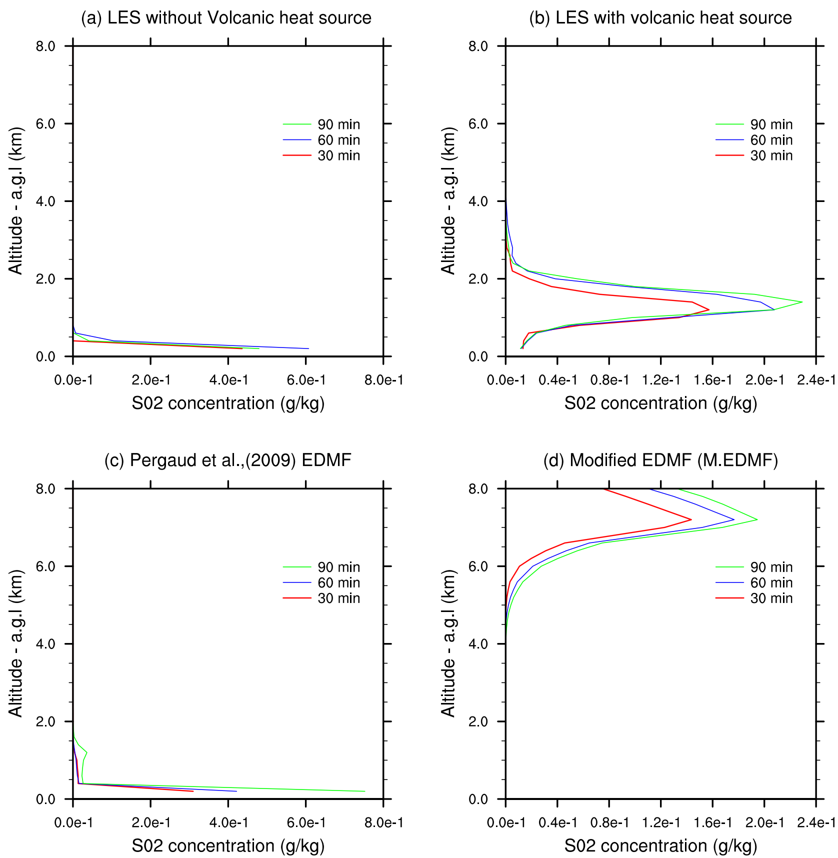

Figure 5. Horizontally averaged SO_2 tracer concentrations ($g\,kg^{-1}$) over 100×100 points for **(a)** and **(b)**; SO_2 concentrations ($g\,kg^{-1}$) in the central grid cell of the SCM simulations for **(c)** and **(d)**. All simulations were inputted with the same SO_2 concentration at the first model level. Red – 30 min, blue – 60 min, green – 90 min after model initialisation.

GMDD
7, 8361–8397, 2014

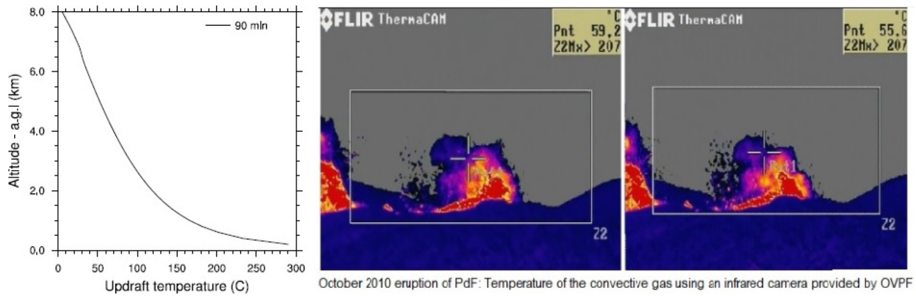

Figure 6. Updraft temperature (°C) of Fig. 5d at 90 min (left). Temperature (°C) of October 2010 eruption of PdF through infrared imagery provided by OVPF. The point at 55–59 °C indicated in the figure is at about 20 m above the crater rim.

GMDD
7, 8361–8397, 2014

Title Page
Abstract Introduction
Conclusions References
Tables Figures
◀ ▶
Back Close
Full Screen / Esc
Printer-friendly Version
Interactive Discussion

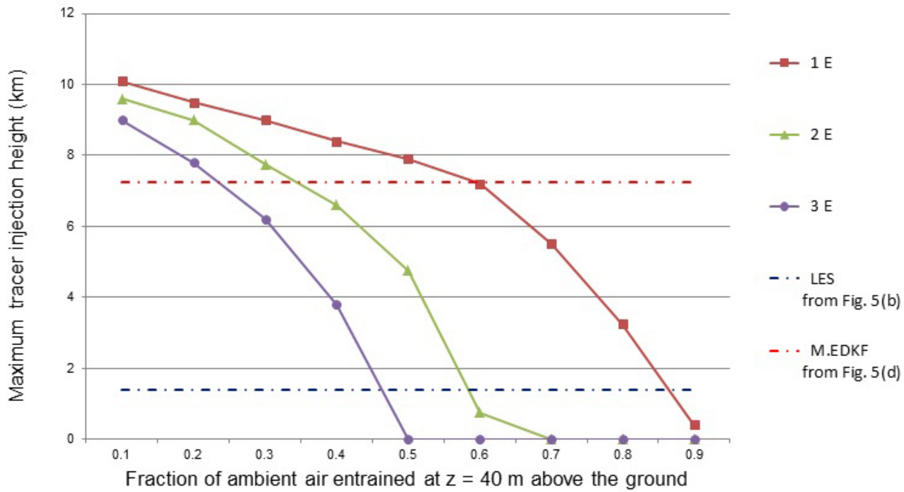

Figure 7. Sensitivity of maximum injection height of tracer to various percentages of ambient air entrained into the buoyant plume in the first model level ($\Delta z = 40$ m a.g.l.). Red dashed line shows the maximum injection height obtained from Fig. 5d and dashed black line shows the maximum injection height as obtained from Fig. 5b. Legends "1E, 2E and 3E" refer to experiments performed whereby the entrainment and detrainment rates are modified in the first model level (see Sects. 2.2.3 and 3.2 for details).

GMDD
7, 8361–8397, 2014

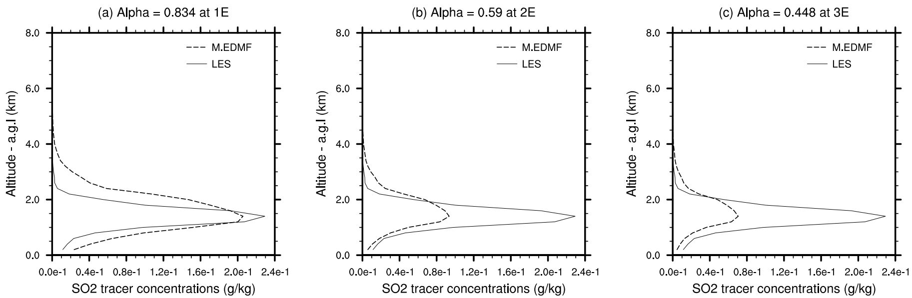

Figure 8. SO_2 tracer concentrations ($g\,kg^{-1}$) and maximum injection height (km a.g.l.) for certain values of α used and ε/δ distribution (1E, 2E, 3E) in the first model level ($\Delta z = 40$ m) at 90 min. LES (solid lines) and M.EDMF (dashed lines).

GMDD
7, 8361–8397, 2014

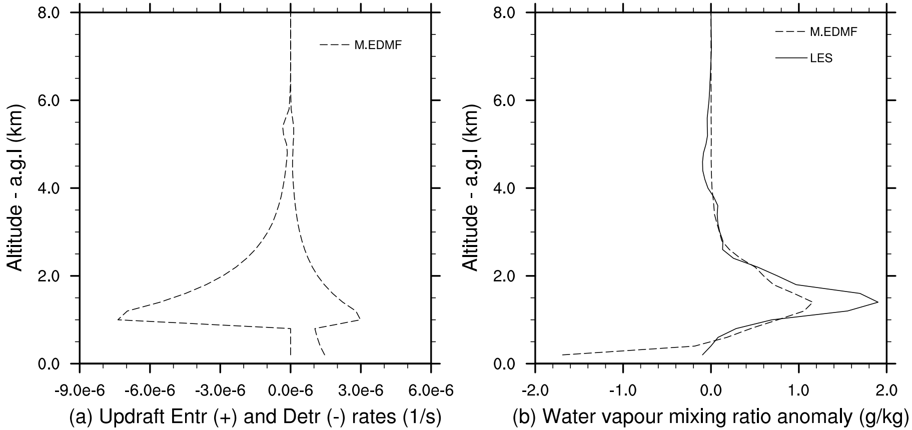

Figure 9. (a) Updraft entrainment (positive values) and detrainment (negative values) rates displayed from the M.EDMF model at 90 min of simulation time (simulation run using $\alpha = 0.834$ at 1E). **(b)** Water vapour mixing ratio (q_u) anomaly ($g\,kg^{-1}$) i.e. q_u (t_{90}) – q_u (t_0), where t_0 and t_{90} is simulation time at 0 and 90 min respectively. LES (solid line) and M.EDMF (dashed lines).